

Deterministic and Probabilistic Rounding Error Analysis for Mixed-Precision Arithmetic on Modern Computing Units

Sahil Bhola, Karthik Duraisamy

*Department of Aerospace Engineering & Michigan Institute for Computational Discovery and Engineering,
University of Michigan, Ann Arbor, U.S.A.*

Abstract

Modern computer architectures support low-precision arithmetic, which present opportunities for the adoption of mixed-precision algorithms to achieve high computational throughput and reduce energy consumption. As a growing number of scientific computations leverage specialized hardware accelerators, the risk of rounding errors increases, potentially compromising the reliability of models. This shift towards hardware-optimized, low-precision computations highlights the importance of rounding error analysis to ensure that performance gains do not come at the expense of accuracy, especially in high-stakes scientific applications. In this work, we conduct rounding error analysis on widely used operations such as fused multiply-add (FMA), mixed-precision FMA (MPFMA), and NVIDIA Tensor cores. We present a deterministic and probabilistic approach to quantifying the accumulated rounding errors. Numerical experiments are presented to perform the multiply and accumulate operation (MAC) and matrix-matrix multiplication using Tensor cores with random data. We show that probabilistic bounds produce tighter estimates by nearly an order of magnitude compared to deterministic ones for matrix-matrix multiplication.

1. Introduction

Rapidly growing computational demands of artificial intelligence workloads have fundamentally reshaped hardware architectures, introducing specialized accelerators and novel arithmetic formats optimized for neural network operations. This transformation of the hardware landscape requires a corresponding evolution in scientific computing paradigms to effectively utilize these architectures. Double precision `fp64` has been the default choice for applications in science and engineering. Recently, an increasing number of applications such as deep learning [1, 2, 3], climate modeling [4, 5, 6], solution of linear systems of equations [7, 8, 9, 10, 11], fluid dynamics [12, 13, 14], and natural sciences [15] have begun leveraging low- or mixed-precision arithmetic for better performance. However, with improved computational performance comes a dramatic drop in computational accuracy as rounding errors become prominent with low-precision arithmetic. This warrants that any application leveraging low- or mixed-precision arithmetic must be aware of the accumulated rounding error to ensure that performance gains are not obtained at the expense of accuracy.

Traditional deterministic rounding error analysis (DBEA) assumes the worst-case scenario, where the absolute rounding errors are identical to the unit roundoff u [16]. This approach produces error bounds that depend on the constant $\gamma_n \triangleq nu/(1 - nu)$ that holds for $nu < 1$, where n is the number of arithmetic operations. Despite providing strong guarantees, DBEA dramatically overestimates the error for large-scale problems using low-precision arithmetic. This results in a conservative selection of precision. Probabilistic treatment of rounding error can account for the potential cancellation and magnification of rounding errors and therefore provide better estimates of the accumulated rounding error [17, 18, 19, 20, 21]. Previous studies [22, 23] have shown that by treating the rounding error as independent and identically distributed (i.i.d.) random variables, we can obtain error bounds that depend on the constant $\tilde{\gamma}_n \propto \sqrt{n} \forall n$. As a result, probabilistic models scale well with problem size and can, therefore, provide better estimates of the accumulated rounding errors for large-scale problems.

This work examines the fused-multiply and accumulate (FMA), mixed-precision fused-multiply and accumulate (MPFMA), and matrix-matrix multiplication using Tensor Cores (TCs). These kernels are widely used in numerical linear algebra as building blocks for kernels such as dot-products, block LU

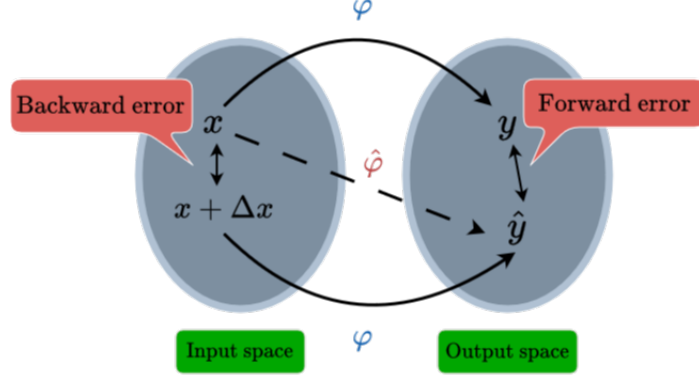


Figure 1: Schematic of backward and forward errors. Solid line: exact; dashed line: computed.

factorization, and Cholesky factorization. We present both the deterministic and probabilistic rounding analysis for these kernels.

The manuscript is organized as follows. In section 2, the rounding error due to floating-point representation and its interpretation using backward and forward errors is presented. In section 3, we perform deterministic and probabilistic rounding error analysis for FMA, MPFMA, and matrix-matrix multiplication using TCs. In section 4, the numerical experiments are presented for the multiply and accumulate operation and performing matrix-matrix multiplication. In section 5, we present the concluding remarks for this work and provide future directions.

2. Floating-point Arithmetic

For a given *precision* $p \in \mathbb{N}$, *base* β , and *exponent range* $e_{\min} \leq e \leq e_{\max}$, we can define the floating point number system $\mathbb{F} \subset \mathbb{R}$ as

$$\mathbb{F} \triangleq \left\{ (-1)^s d_0.d_1d_2 \dots d_{p-1} \times \beta^e \mid s \in \{0, 1\}, 0 \leq d_i \leq \beta - 1 \right\}, \quad (1)$$

where $d_0 \neq 0$ for normalized numbers. Given the tuple $t^* \triangleq (p, \beta, e_{\min}, e_{\max})$, a finite and unique set of *representable* numbers can be obtained that constitute the floating-point system. Standard floating-point systems include IEEE half (fp16), single (fp32), and double (fp64) precision, for which the tuple parameters are tabulated in table 1. Thus, representing $z \in \mathbb{R}$ in a floating-point system requires a *rounding operation* $fl : \mathbb{R} \rightarrow \mathbb{F}$ that maps z to a floating-point representable number according to a rounding model. Due to this rounding operation, there is a loss of information (or bits) that introduces a *rounding error*, which can grow with successive floating point operations. Thus, computing any real-valued function $\varphi : \mathbb{R}^{n_{in}} \rightarrow \mathbb{R}^{n_{out}}$ in finite-precision produces an approximate $\hat{\varphi} : \mathbb{F}^{n_{in}} \rightarrow \mathbb{F}^{n_{out}}$, as illustrated in fig. 1. To quantify the approximation quality, we can then define *forward error* as the absolute or relative error specified in the output space. Alternatively, the effect of rounding can be understood as perturbations to the input space that propagate through the true function. To this end, we can define a perturbation $\Delta \mathbf{x}$ to the input space \mathbf{x} , such that $\varphi(\mathbf{x} + \Delta \mathbf{x}) = \hat{\varphi}(\mathbf{x})$. Since the input perturbation can be non-unique, we can define the smallest relative perturbation called the *backward error* as the solution of the optimization problem

$$\epsilon_{bwd} \triangleq \min\{\epsilon \geq 0 : \hat{\varphi}(\mathbf{x}) = \varphi(\mathbf{x} + \Delta \mathbf{x}), |\Delta \mathbf{x}| \leq \epsilon |\mathbf{x}|\}. \quad (2)$$

Forward or backward error bounds can be developed to quantify the rounding uncertainty. In this work, we focus on developing backward error bounds, which can be directly compared with uncertainties in the input space. This is useful because for a given floating-point system parameterized by t^* , if the inherent uncertainty in the input space is larger than the backward error, then the computed solution can be considered reliable. Further, backward error bounds can also be used to develop forward error bounds that are useful for uncertainty propagation.

2.1. Rounding Error Analysis

The rounding uncertainty resulting from finite-precision approximation implicitly depends on the rounding operations. Using the IEEE standard [24], the rounding operation can be modeled as

$$fl(z) \triangleq z(1 + \delta)^\rho; \quad z \in \mathbb{R}, \rho = \pm 1, |\delta| \leq u \quad (3)$$

where δ is the *rounding error*, and $u \triangleq \frac{1}{2}\beta^{1-p}$ is the *unit roundoff*. Thus, the rounding error terms accumulate when computing the true function φ in finite precision. For example, evaluating $y = \sum_{i=1}^3 x_i$ in finite precision results in an approximation $\hat{y} = \sum_{i=1}^3 x_i(1 + \eta_i) \prod_{j=\max(2,i)}^3 (1 + \delta_j)$, assuming recursive summation from left-to-right. Here, η_i is due to the rounding $fl(x_i)$, and δ_i arises due to the rounding after the addition operation. In backward error analysis, a bound for the product $\prod_{i=1}^n (1 + \delta_i)$ is sought to obtain a perturbed system.

Deterministic Backward Error Analysis (DBEA). In the traditional backward analysis, the following lemma [16, Lemma 3.1] is used to bound the distance between 1 and the product $\prod_{i=1}^n (1 + \delta_i)^{\rho_i}$.

Lemma 2.1 (Deterministic rounding error bound). *If $|\delta_i| \leq u$ and $\rho_i = \pm 1$ for $i = 1, \dots, n$, and $nu < 1$, then*

$$\prod_{i=1}^n (1 + \delta_i)^{\rho_i} \triangleq 1 + \theta_n^u,$$

with $|\theta_n^u| \leq \gamma_n^u \triangleq \frac{nu}{1-nu}$.

Variance-informed Probabilistic Backward Error Analysis (VIBE). While the traditional deterministic analysis provides strong guarantees for the rounding uncertainty, it considers the worst-case scenario where the absolute rounding error is identical to the unit roundoff. This dramatically overestimates the accumulated rounding errors, producing very pessimistic error bounds —especially when using low-precision arithmetic for a large number of operations. To address this, [23, Theorem 3.4] proposed the following lemma.

Lemma 2.2 (Variance-informed probabilistic error bounds). *Let $\delta_1, \dots, \delta_n$ represent n i.i.d. random variables distributed uniformly as $\mathcal{U}[-u, u]$ where $u \leq 1$. Then for $\lambda \geq 0$*

$$\prod_{i=1}^n (1 + \delta_i)^{\rho_i} = 1 + \tilde{\theta}_n^u,$$

hold such that $|\tilde{\theta}_n^u| \leq \tilde{\gamma}_n^u(\lambda)$ with probability at least

$$p_b(\lambda, u, n) \triangleq 1 - 2 \exp\left(\frac{-\lambda^2 nu^2}{2(\sigma^2 + \frac{\lambda \sqrt{nu^2}}{3(1-u)})}\right),$$

where

$$\sigma^2 = n \left(\frac{4u^2 + \kappa(\log(1-u)^2 - 2\log(1-u)\log(1+u) + \log(1+u)^2)}{4u^2} \right),$$

with $\kappa = (-1 + u^2)$.

Arithmetic	p	β	e_{\min}	e_{\max}
IEEE half (fp16)	11	2	-14	15
IEEE single (fp32)	24	2	-126	127
IEEE double (fp64)	53	2	-1022	1023

Table 1: Floating point arithmetic parameters for IEEE standard.

3. Application to Numerical Linear Algebra

In this section we first present the backward error bounds for the fused multiply-add (FMA) operation, mixed-precision FMA (MPFMA) operation. Followed by, we extend the MPFMA backward error bounds to obtain the backward-forward error bounds for the NVIDIA Tensor Core operations.

3.1. Fused Multiply-Add (FMA)

The FMA operation is a hardware-level instruction defined as $fma(a, b, c)$, computed as the correctly rounded exact result $fl_u(a \times b + c)$. Due to fewer rounding operations and, thereby, smaller rounding errors, these operations are widely used in numerical algorithms such as computing dot products, generalized matrix-matrix multiplications (GEMM), and polynomial evaluations. For example, computing the dot-product $z = \sum_{i=1}^n x_i y_i$ via recursive summation requires n multiplications and $n - 1$ summations. Alternatively, we can compute the dot-product as a recursive FMA operation $s_i = fma(x_i, y_i, s_{i-1})$ for $i = 1 \dots n$, where $s_0 = 0$ and $z = s_n$. In this section, we study the backward error bounds for the FMA operation.

3.1.1. Deterministic Analysis

Lemma 3.1 (FMA without representation error). *Let the multiply-accumulate operation $z = a \times b + c$ be evaluated using the FMA operation, where $a, b, c \in \mathbb{F}$ characterized by the tuple t^* with a unit roundoff u . Under the IEEE arithmetic model and lemma 2.1, the computed approximation \hat{z} satisfies*

$$\hat{z} = a \times (b + \Delta b) + (c + \Delta c) = (a + \Delta a) \times b + (c + \Delta c),$$

where $|\Delta a| \leq u|a|$, $|\Delta b| \leq u|b|$, and $|\Delta c| \leq u|c|$.

Proof. The approximation \hat{z} is the correctly rounding exact result given as

$$\begin{aligned} \hat{z} &= fma(a, b, c)(1 + \delta) = (a \times b + c)(1 + \delta); \quad |\delta| \leq u, \\ &= (a \times b)(1 + \delta) + c(1 + \delta), \\ &= a \times (b + \Delta b) + (c + \Delta c) = (a + \Delta a) \times b + (c + \Delta c), \end{aligned}$$

where $|\Delta a| \triangleq |a\delta| \leq u|a|$, $|\Delta b| \triangleq |b\delta| \leq u|b|$, and $|\Delta c| \triangleq |c\delta| \leq u|c|$. □

Using lemma 3.1, we can then obtain the relative forward error bound as

$$\frac{|\hat{z} - z|}{|z|} \leq u \frac{|a| \times |b| + |c|}{|a \times b + c|}. \quad (4)$$

If a, b , and c are described by the tuple t^* with a unit roundoff $u < u$, where u is the unit roundoff for the FMA operation, then we must account for the initial change in precision. Using lemma 2.1

$$\tilde{z} = a \times (b + \Delta b) + c + \Delta c, \quad |\Delta b| \leq \gamma_2^u |b|; |\Delta c| \leq u|c|,$$

which is the expression that is then computed using the FMA operation. Using lemma 3.1, the computed approximation satisfies

$$\begin{aligned} \hat{z} &= a \times (b + \Delta b + \Delta(b + \Delta b)) + (c + \Delta c) + \Delta(c + \Delta c), \\ &= a \times b + c + a\Delta b + a\Delta(b + \Delta b) + \Delta c + \Delta(c + \Delta c), \\ &\triangleq a \times b + c + \Delta p, \end{aligned}$$

where $|\Delta(b + \Delta b)| \leq u|b + \Delta b|$ and $|\Delta(c + \Delta c)| \leq u|c + \Delta c|$. We can then bound Δp to obtain the forward error bound as stated in lemma 3.2.

Lemma 3.2 (FMA with representation error). *Let the multiply-accumulate operation $z = a \times b + c$ be evaluated using the FMA operation with a unit roundoff u , where $a, b, c \in \mathbb{F}$ characterized by the tuple t^* with a unit roundoff $u < u$. Under the IEEE arithmetic model and lemma 2.1, the computed approximation \hat{z} satisfies*

$$\frac{|\hat{z} - z|}{|z|} \leq \frac{(u + \gamma_2^u + u\gamma_2^u)|a| \times |b| + (2u + u^2)|c|}{|a \times b + c|}.$$

3.1.2. Probabilistic Analysis

It is trivial to show that for an FMA operation without representation error, DBEA and VIBEA result in the same backward error bound, which always holds. In the case there is an initial change in precision, we can use lemma 2.2 to obtain

$$\tilde{z} = a \times (b + \Delta b) + c + \Delta c,$$

where $|\Delta b| \leq \tilde{\gamma}_2^u |b|$ holds with probability at least $p_b(\lambda, u, 2)$ and $|\Delta c| \leq u|c|$. Following section 3.1.1, the probabilistic forward error bounds can be obtained as stated in lemma 3.3.

Lemma 3.3 (FMA with representation error). *Let the multiply-accumulate operation $z = a \times b + c$ be evaluated using the FMA operation with a unit roundoff u , where $a, b, c \in \mathbb{F}$ characterized by the tuple t^* with a unit roundoff $\hat{u} < u$. Under the IEEE arithmetic model and lemma 2.2, the computed approximation \hat{z} satisfies*

$$\frac{|\hat{z} - z|}{|z|} \leq \frac{(u + \tilde{\gamma}_2^u + u\tilde{\gamma}_2^u)|a| \times |b| + (2u + u^2)|c|}{|a \times b + c|},$$

with a probability at least $p_b(\lambda, u, 2)$.

3.2. Mixed-precision FMA (MPFMA)

While the FMA operation presented in section 3.1 delivers performance optimization via hardware-level instructions, it is typically performed with a fixed precision. Modern hardware provides a dictionary of lower precision, such as **fp4** and **fp8**, that can be leveraged to reduce the memory bandwidth requirement and attain high throughput. The typical MPFMA operation takes in the input a and b in

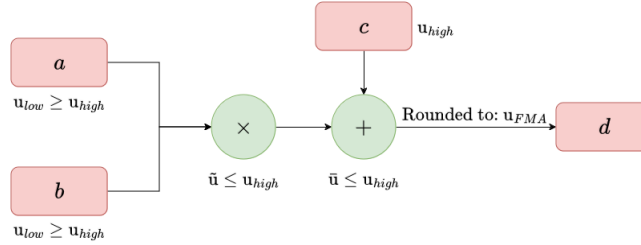


Figure 2: Schematic of the mixed-precision FMA operation.

a lower precision characterized by the tuple t_{low} with a unit roundoff u_{low} , and c in a higher precision characterized by the tuple t_{high} with unit roundoff u_{high} . This is illustrated in fig. 2. The product $a \times b$ is performed in a higher precision characterized by the tuple \tilde{t} , with a unit roundoff $\tilde{u} \leq u_{high}$. To ensure that this product does not introduce any rounding error, the low precision floating point system t_{low} is chosen to represent the entire significant of the product in the floating point system \tilde{t} . For example, the NVIDIA tensor cores utilize **fp16** as the low precision and compute the product in **fp32**. The product of two **fp16** has at most 20 significant bits, which can be entirely represented by the 23 significant bits of **fp32**. Following the product, the accumulation operation is performed in the floating point system \tilde{t} – introducing a rounding error. Lastly, the output is stored in a floating point system characterized by t_{FMA} with a unit roundoff u_{FMA} . If $u_{FMA} > \tilde{u}$, then this step also introduces a rounding error. In this section, we present the backward error analysis of the MPFMA operation.

3.2.1. Deterministic Analysis

Lemma 3.4 (MPFMA without representation error). *Let the multiply-accumulate operation $z = a \times b + c$ be evaluated using MPFMA operation, where $ab \in \mathbb{F}$ characterized by the tuple t_{low} and $c \in \mathbb{F}$ characterized by the tuple t_{high} . Consider that the multiply and accumulate operation is performed in a floating point system characterized by \tilde{t} (with unit roundoff \tilde{u}) and \tilde{t} (with unit roundoff \tilde{u}), respectively. Let the output unit roundoff be given as $u_{FMA} > \tilde{u}$. Then, under the IEEE arithmetic model and lemma 2.1, the computed approximation \hat{z} to z satisfies*

$$\hat{z} = a \times (b + \Delta b) + (c + \Delta c) = (a + \Delta a) \times b + (c + \Delta c),$$

where

$$\begin{aligned} |\Delta a| &\leq (\bar{u} + u_{FMA} + \bar{u}u_{FMA})|a|, \\ |\Delta b| &\leq (\bar{u} + u_{FMA} + \bar{u}u_{FMA})|b|, \\ |\Delta c| &\leq (\bar{u} + u_{FMA} + \bar{u}u_{FMA})|c|. \end{aligned}$$

Proof. Assume that the significant of the product $a \times b$ can be entirely represented by the significant of the floating point system \tilde{t} . Then, the computed approximation is given as

$$\begin{aligned} \hat{z} &= (a \times b + c)(1 + \delta)(1 + \eta), \quad |\delta| \leq \bar{u}, |\eta| \leq u_{FMA}, \\ &= a \times (b + \Delta b) + (c + \Delta c) = (a + \Delta a) \times b + (c + \Delta c), \end{aligned}$$

where $\Delta a \triangleq (\delta + \eta + \delta\eta)a$, $\Delta b \triangleq (\delta + \eta + \delta\eta)b$ and $\Delta c \triangleq (\delta + \eta + \delta\eta)c$. This gives

$$\begin{aligned} |\Delta a| &\leq (\bar{u} + u_{FMA} + \bar{u}u_{FMA})|a|, \\ |\Delta b| &\leq (\bar{u} + u_{FMA} + \bar{u}u_{FMA})|b|, \\ |\Delta c| &\leq (\bar{u} + u_{FMA} + \bar{u}u_{FMA})|c|. \end{aligned}$$

□

Using lemma 3.4, the relative forward error bound is given as

$$\frac{|\hat{z} - z|}{|z|} \leq (\bar{u} + u_{FMA} + \bar{u}u_{FMA}) \frac{|a| \times |b| + |c|}{|a \times b + c|}. \quad (5)$$

In the special case where $\bar{u} = \bar{u} = u_{FMA} = u_{high}$, there is only a single rounding operation, such that the computed approximation becomes

$$\hat{z} = a \times (b + \Delta b) + (c + \Delta c) = (a + \Delta a) \times b + (c + \Delta c),$$

where $|\Delta b| \leq u_{high}$ and $|\Delta c| \leq u_{high}$. This results in a forward error bound

$$\frac{|\hat{z} - z|}{|z|} \leq u_{high} \frac{|a| \times |b| + |c|}{|a \times b + c|}, \quad (6)$$

which is identical to the bound obtained when performing an FMA operation, as shown in lemma 3.1.

If a, b, c are described by the tuple t^* with unit roundoff $\bar{u} < u_{high}$, then the initial change in precision must also be accounted for. Using lemma 2.1, we can obtain

$$\tilde{z} = a \times (b + \Delta b) + c + \Delta c, \quad |\Delta b| \leq \gamma_2^{u_{low}}; |\Delta c| \leq u_{high}|c|,$$

which is the expression that is then computed using MPFMA. Using lemma 3.4, the computed approximation then satisfies

$$\begin{aligned} \hat{z} &= a \times (b + \Delta b + \Delta(b + \Delta b)) + (c + \Delta c) + \Delta(c + \Delta c), \\ &\triangleq a \times b + c + \Delta p, \end{aligned}$$

where $|\Delta(b + \Delta b)| \leq (\bar{u} + u_{FMA} + \bar{u}u_{FMA})|b + \Delta b|$, $|\Delta(c + \Delta c)| \leq (\bar{u} + u_{FMA} + \bar{u}u_{FMA})|c + \Delta c|$, and $\Delta p \triangleq a\Delta b + a\Delta(b + \Delta b) + \Delta c + \Delta(c + \Delta c)$. We can then bound Δp to obtain the forward error bound, as stated in lemma 3.5.

Lemma 3.5 (MPFMA with representation error). *Let the multiply-accumulate operation $z = a \times b + c$ be evaluated using MPFMA operation, where a, b and c are characterized by the tuple t^* with unit roundoff $\bar{u} < u_{high}$. Consider that the multiply and accumulate operation is performed in a floating point system characterized by \tilde{t} (with unit roundoff \bar{u}) and \bar{t} (with unit roundoff \bar{u}), respectively. Let the output unit roundoff be given as $u_{FMA} > \bar{u}$. Then, under the IEEE arithmetic model and lemma 2.1, the computed approximation \hat{z} to z satisfies*

$$\frac{|\hat{z} - z|}{|z|} \leq \frac{[\gamma_2^{u_{low}} + \zeta(1 + \gamma_2^{u_{low}})]|a||b| + [u_{high} + \zeta(1 + u_{high})]|c|}{|a \times b + c|},$$

where $\zeta \triangleq \bar{u} + u_{FMA} + \bar{u}u_{FMA}$.

3.2.2. Probabilistic Analysis

It is trivial to show that VIBEa results in the same backward and forward error bounds for MPFMA without any representation error, which always holds. In the case there is precision change, we can use lemma 2.2 to obtain

$$\tilde{z} = a \times (b + \Delta b) + (c + \Delta c),$$

where $|\Delta b| \leq \tilde{\gamma}_2^{u_{low}}$ holds with probability $p_b(\lambda, u_{low}, 2)$ and $|\Delta c| \leq u_{high}|c|$. Following section 3.2.1, the probabilistic backward error bounds can be obtained as stated in lemma 3.6.

Lemma 3.6 (MPFMA with representation error). *Let the multiply-accumulate operation $z = a \times b + c$ be evaluated using MPFMA operation, where a, b and c are characterized by the tuple t^* with unit roundoff $\bar{u} < u_{high}$. Consider that the multiply and accumulate operation is performed in a floating point system characterized by \tilde{t} (with unit roundoff \tilde{u}) and \bar{t} (with unit roundoff \bar{u}), respectively. Let the output unit roundoff be given as $u_{FMA} > \bar{u}$. Then, under the IEEE arithmetic model and lemma 2.2, the computed approximation \hat{z} to z satisfies*

$$\frac{|\hat{z} - z|}{|z|} \leq \frac{[\tilde{\gamma}_2^{u_{low}} + \zeta(1 + \tilde{\gamma}_2^{u_{low}})]|a||b| + [u_{high} + \zeta(1 + u_{high})]|c|}{|a \times b + c|},$$

with a probability at least $p_b(\lambda, u_{low}, 2)$, where $\zeta \triangleq \bar{u} + u_{FMA} + \bar{u}u_{FMA}$.

3.3. Tensor Cores (TCs)

Tensor cores were introduced in the NVIDIA Volta architecture as dedicated hardware to perform MPFMA on matrices. They are designed to perform the operation $\mathbf{D} = \mathbf{C} + \mathbf{A}\mathbf{B}$, where $\mathbf{C} \in \mathbb{R}^{b_1 \times b_2}$, $\mathbf{A} \in \mathbb{R}^{b_1 \times b}$, and $\mathbf{B} \in \mathbb{R}^{b \times b_2}$ in a single clock cycle for $b_1 = b_2 = b = 4$. To perform MPFMA, TCs take the input matrix \mathbf{A}, \mathbf{B} in a lower precision (with unit roundoff u_{low}) and the accumulator \mathbf{C} in a higher precision (with unit roundoff $u_{high} \leq u_{low}$). Each TC performs 64 MPFMA operations (16 dot products of vector of size 4) with a multiply operation in a floating point system \tilde{t} (with unit roundoff \tilde{u}) and an accumulation in the system \bar{t} (with unit roundoff \bar{u}), as illustrated in fig. 3. The NVIDIA programming guide states

Element-wise multiplication of matrix \mathbf{A} and \mathbf{B} is performed with at least single precision. When .ctype or .dtype is .f32, accumulation of the intermediate values is performed with at least a single precision. When both .ctype and .dtype are specified as .f16, the accumulation is performed with at least half precision.

To this end, we summarize the unit roundoff utilized by TCs in table 2. As discussed in section 3.2, the choice of \bar{u} ensures that multiplication does not introduce any error. This means that while the present architecture is designed to handle matrices \mathbf{A} and \mathbf{B} in **fp16**, there is a scope for further quantization. TCs are particularly useful as they can efficiently multiply matrix-matrix by decomposing the output matrix into smaller blocks, as described in algorithm 1.

[25] presented a general framework to perform deterministic backward error analysis for algorithm 1. In this work, we first consider a special case wherein the choice of \tilde{t} ensures that the multiply does not introduce any rounding error. In this section, under this assumption, we first re-derive the deterministic analysis of [25]. Following this, we present a probabilistic backward error analysis for TCs.

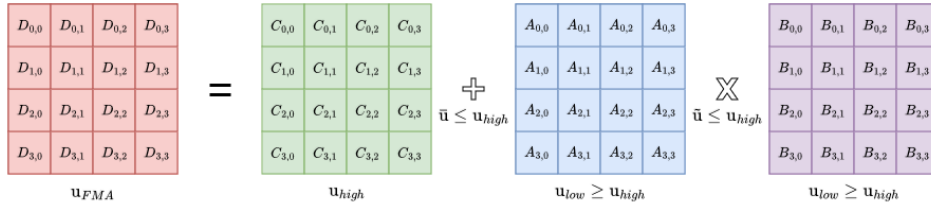


Figure 3: Schematic for Tensor core matrix multiply and accumulate.

Algorithm 1 Let $\mathbf{D} = \mathbf{AB}$, where $\mathbf{A} \in \mathbb{R}^{m \times n}$ and $\mathbf{B} \in \mathbb{R}^{n \times t}$ be computed using Tensor cores by partitioning the output matrix \mathbf{D} into smaller blocks of size $b_1 \times b_2$ (denoted as D_{ij}). Assume that $m \triangleq pb_1$, $n \triangleq qb$, and $t \triangleq rb_2$, where $p, q, r \in \mathbb{Z}_{\geq 1}$. The block $\mathbf{D}_{ij} \triangleq \sum_{k=1}^q \mathbf{A}_{ik} \mathbf{B}_{kj}$, where \mathbf{A}_{ik} and \mathbf{B}_{kj} denotes a block of \mathbf{A} and \mathbf{B} of size $b_1 \times b$ and $b \times b_2$, respectively. Consider that \mathbf{A}, \mathbf{B} are stored in the floating point system t_{low} with unit roundoff u_{low} . Consider that the multiplication and accumulation are performed in the floating point system \tilde{t} (with unit roundoff \tilde{u}) and \bar{t} (with unit roundoff \bar{u}), respectively. The output unit roundoff is u_{FMA} .

```

 $\tilde{\mathbf{A}} \leftarrow fl_{u_{low}}(\mathbf{A})$  and  $\tilde{\mathbf{B}} \leftarrow fl_{u_{low}}(\mathbf{B})$ .
for  $i = 1$  to  $p$  do
  for  $j = 1$  to  $r$  do
     $\mathbf{D}_{ij} \leftarrow \mathbf{0}$ .
    for  $k = 1$  to  $q$  do
      Compute  $\mathbf{D}_{ij} \leftarrow fl_{u_{FMA}}(\mathbf{D}_{ij} + \tilde{\mathbf{A}}_{ik} \tilde{\mathbf{B}}_{kj})$ 
    end for
  end for
end for

```

A	B	C	D	u_{low}	u_{high}	\tilde{u}	\bar{u}	u_{FMA}
fp16	fp16	fp32	fp32	u_{fp16}	u_{fp32}	u_{fp32}	u_{fp32}	u_{fp32}
fp16	fp16	fp16	fp16	u_{fp16}	u_{fp16}	u_{fp32}	u_{fp16}	u_{fp16}

Table 2: Unit roundoff for Tensor Cores

3.3.1. Deterministic Analysis

Tensor cores recursively utilize the kernel $z_i = z_{i-1} + \sum_{j=1}^b x_j y_j$, where x_i, y_j are given in the system t_{low} and z_{i-1} is given in the system t_{high} . Multiplications and accumulations are performed in \tilde{t} and \bar{t} , respectively; output z_i is in the floating point system t_{FMA} . An illustration of how this kernel is utilized is shown in fig. 4. Under the assumption that performing the multiplication in \tilde{t} does not

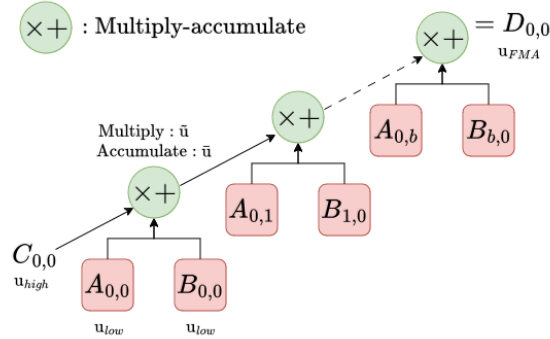


Figure 4: An illustration of the Tensor core kernel.

introduce any additional error, we can use lemma 2.1 to obtain the computed approximation

$$\hat{z}_i = \left(z_{i-1} \prod_{k=1}^b (1 + \delta_k) + \sum_{j=1}^b x_j y_j \prod_{k=j}^b (1 + \delta_k) \right) (1 + \eta_i); \quad |\delta_k| \leq \bar{u}, |\eta_i| \leq u_{FMA}, \quad (7)$$

assuming left-to-right computation. If \mathbf{x} denotes a row of $\tilde{\mathbf{A}}$ and \mathbf{y} denotes the $\tilde{\mathbf{B}}$, then using algorithm 1 an element of the output matrix \mathbf{D} is given as

$$s_n \triangleq \underbrace{\mathbf{x}^T \mathbf{y}}_{\text{Computed in blocks of size } b},$$

$$= \sum_{i=1}^q \sum_{j=(i-1)b+1}^{ib} x_j y_j,$$

Using eq. (7), the computed approximation \hat{s}_n is given as

$$\hat{s}_n = \sum_{i=1}^q \left(\sum_{j=(i-1)b+1}^{ib} x_j y_j \prod_{k=((j-1) \bmod b)+1}^b (1 + \delta_k^{(i)}) \right) \overbrace{\prod_{\ell=\max(2,i)}^q \prod_{\kappa=1}^b (1 + \delta_{\kappa}^{(\ell)})}^{\text{Adding previous block}} \underbrace{\prod_{\varrho=i}^q (1 + \eta_{\varrho})}_{\text{Conversion to } t_{FMA}},$$

where $|\delta_k^{(i)}|, |\delta_k^{(\ell)}| \leq \bar{u}$, $|\eta_{\ell}| \leq u_{FMA}$, and $\delta_{k=1}^{i=1} = 0$ (adding to 0 does not introduce any error). Using lemma 2.1 and [16, Lemma 3.3]

$$\begin{aligned} \hat{s}_n &= \sum_{i=1}^q \left(\sum_{j=(i-1)b+1}^{ib} x_j y_j (1 + \theta_{b-((j-1) \bmod b)}^{\bar{u}(i)}) \right) (1 + \theta_{b*(q-\max(2,i)+1)}^{\bar{u}}) (1 + \theta_{q-i+1}^{u_{FMA}}), \\ &= \sum_{i=1}^q \sum_{j=(i-1)b+1}^{ib} x_j y_j (1 + \theta_{b-((j-1) \bmod b)+b*(q-\max(2,i)+1)}^{\bar{u}(i)}) (1 + \theta_{q-i+1}^{u_{FMA}}), \end{aligned}$$

where $|\theta_{\zeta}^{\bar{u}}| \leq \gamma_{\zeta}^{\bar{u}}$ and $|\theta_{\zeta}^{u_{FMA}}| \leq \gamma_{\zeta}^{u_{FMA}}$. Thus,

$$\hat{s}_n = \sum_{i=1}^q \sum_{j=(i-1)b+1}^{ib} x_j (y_j + \Delta y_j),$$

where $\Delta y_j \triangleq (\theta_{b-((j-1) \bmod b)+b*(q-\max(2,i)+1)}^{\bar{u}(i)} + \theta_{q-i+1}^{u_{FMA}} + \theta_{b-((j-1) \bmod b)+b*(q-\max(2,i)+1)}^{\bar{u}(i)} * \theta_{q-i+1}^{u_{FMA}}) y_j$, such that

$$|\Delta y_j| \leq |\theta_{b-((j-1) \bmod b)+b*(q-\max(2,i)+1)}^{\bar{u}(i)}| + |\theta_{q-i+1}^{u_{FMA}}| + |\theta_{b-((j-1) \bmod b)+b*(q-\max(2,i)+1)}^{\bar{u}(i)}| |\theta_{q-i+1}^{u_{FMA}}| |y_j|$$

which can be upper bounded for $i = j = 1$ (for which $\theta_{\zeta}^{\bar{u}}$ is effectively $\theta_{\zeta-1}^{\bar{u}}$ since $\delta_{j=1}^{i=1} = 0$) as

$$|\Delta y_j| \leq (\gamma_{n-1}^{\bar{u}} + \gamma_q^{u_{FMA}} + \gamma_{n-1}^{\bar{u}} * \gamma_q^{u_{FMA}}) |y_j|.$$

This gives the forward error in computing an element of \mathbf{D} as

$$\frac{|\hat{s}_n - s_n|}{|s_n|} \leq (\gamma_{n-1}^{\bar{u}} + \gamma_q^{u_{FMA}} + \gamma_{n-1}^{\bar{u}} * \gamma_q^{u_{FMA}}) \frac{|\mathbf{x}|^T |\mathbf{y}|}{|\mathbf{x}^T \mathbf{y}|}$$

Compared to [25], we obtain a factor of $n - 1$ due to the assumption of errorless multiplication in the floating point system \tilde{t} .

Using this result, we can obtain the forward error for performing the matrix-matrix multiplication, as stated in theorem 3.7.

Theorem 3.7 (Tensor cores without representation error). *Let $\mathbf{D} = \mathbf{AB}$ be computed using Tensor Cores, where \mathbf{A}, \mathbf{B} are given in the floating point system t_{low} . If algorithm 1 is used to compute the matrix-matrix multiplication, then under lemma 2.1, the computed approximation $\hat{\mathbf{D}}$ satisfies*

$$\frac{|\hat{\mathbf{D}} - \mathbf{D}|}{|\mathbf{D}|} \leq (\gamma_{n-1}^{\bar{u}} + \gamma_q^{u_{FMA}} + \gamma_{n-1}^{\bar{u}} * \gamma_q^{u_{FMA}}) \frac{|\mathbf{A}| |\mathbf{B}|}{|\mathbf{AB}|}.$$

In the case where \mathbf{A} and \mathbf{B} are given in a floating point system t^* with unit roundoff $\bar{u} < u_{low}$, then we must account for the initial change in precision. Using lemma 2.1 we can obtain

$$\tilde{\mathbf{D}} = (\mathbf{A} + \Delta\mathbf{A})(\mathbf{B} + \Delta\mathbf{B}), \quad |\Delta\mathbf{A}| \leq u_{low}|\mathbf{A}|, |\Delta\mathbf{B}| \leq u_{low}|\mathbf{B}|,$$

which is then computed using algorithm 1. This gives the computed approximation to \mathbf{D} as

$$\begin{aligned} \hat{\mathbf{D}} &= (\mathbf{A} + \Delta\mathbf{A})(\mathbf{B} + \Delta\mathbf{B}) + \Delta\mathbf{P}; \quad |\Delta\mathbf{P}| \leq (\gamma_{n-1}^{\bar{u}} + \gamma_q^{u_{FMA}} + \gamma_{n-1}^{\bar{u}} * \gamma_q^{u_{FMA}})|\mathbf{A} + \Delta\mathbf{A}||\mathbf{B} + \Delta\mathbf{B}|, \\ &= \mathbf{AB} + \mathbf{A}\Delta\mathbf{B} + \Delta\mathbf{A}\mathbf{B} + \Delta\mathbf{A}\Delta\mathbf{B} + \Delta\mathbf{P} \\ &\triangleq \mathbf{AB} + \Delta\mathbf{E}, \end{aligned}$$

where $\Delta\mathbf{E} \triangleq \mathbf{A}\Delta\mathbf{B} + \Delta\mathbf{A}\mathbf{B} + \Delta\mathbf{A}\Delta\mathbf{B} + \Delta\mathbf{P}$ which we can bound to obtain the forward error bounds. This is stated in theorem 3.8.

Theorem 3.8 (Tensor cores with representation error). *Let $\mathbf{D} = \mathbf{AB}$ be computed using Tensor Cores, where \mathbf{A}, \mathbf{B} are given in the floating point system t^* with unit roundoff $\bar{u} < u_{low}$. If algorithm 1 is used to compute the matrix-matrix multiplication, then under lemma 2.1, the computed approximation $\hat{\mathbf{D}}$ satisfies*

$$\frac{|\hat{\mathbf{D}} - \mathbf{D}|}{|\mathbf{D}|} \leq (2u_{low} + u^2 + \zeta(1 + u_{low})^2) \frac{|\mathbf{A}||\mathbf{B}|}{|\mathbf{AB}|},$$

where $\zeta \triangleq (\gamma_{n-1}^{\bar{u}} + \gamma_q^{u_{FMA}} + \gamma_{n-1}^{\bar{u}} * \gamma_q^{u_{FMA}})$.

3.3.2. Probabilistic Analysis

Consider the computed \hat{s}_n as

$$\begin{aligned} \hat{s}_n &= \sum_{i=1}^q \left(\sum_{j=(i-1)b+1}^{ib} x_j y_j \prod_{k=((j-1) \bmod b)+1}^b (1 + \delta_k^{(i)}) \right) \prod_{\ell=\max(2,i)}^q \prod_{\kappa=1}^b (1 + \delta_{\kappa}^{(\ell)}) \prod_{\varrho=i}^q (1 + \eta_{\varrho}), \\ &= \sum_{i=1}^q \left(\sum_{j=(i-1)b+1}^{ib} x_j y_j \prod_{k=((j-1) \bmod b)+1}^b (1 + \delta_k^{(i)}) \prod_{\ell=\max(2,i)}^q \prod_{\kappa=1}^b (1 + \delta_{\kappa}^{(\ell)}) \right) \prod_{\varrho=i}^q (1 + \eta_{\varrho}), \\ &= \sum_{i=1}^q \left(\sum_{j=(i-1)b+1}^{ib} x_j y_j (1 + \tilde{\theta}_{b-\{(j-1) \bmod b\}+b*(q-\max(2,i)+1)}^{\bar{u}(i)}) \right) (1 + \tilde{\theta}_{q-i+1}^{u_{FMA}}), \end{aligned}$$

where using lemma 2.2, $|\tilde{\theta}_{\zeta}^{\bar{u}}| \leq \tilde{\gamma}_{\zeta}^{\bar{u}}$ with probability at least $p_b(\lambda, \bar{u}, \zeta)$ and $\tilde{\theta}_{\zeta}^{u_{FMA}} \leq |\tilde{\gamma}_{\zeta}|$ with probability at least $p_b(\lambda, u_{FMA}, \zeta)$. Thus,

$$\hat{s}_n = \sum_{i=1}^q \sum_{j=(i-1)b+1}^{ib} x_j (y_j + \Delta y_j),$$

where $\Delta y_j \triangleq (\theta_{b-\{(j-1) \bmod b\}+b*(q-\max(2,i)+1)}^{\bar{u}(i)} + \theta_{q-i+1}^{u_{FMA}} + \theta_{b-\{(j-1) \bmod b\}+b*(q-\max(2,i)+1)}^{\bar{u}(i)} * \theta_{q-i+1}^{u_{FMA}}) y_j$, such that

$$|\Delta y_j| \leq |\theta_{b-\{(j-1) \bmod b\}+b*(q-\max(2,i)+1)}^{\bar{u}(i)}| + |\theta_{q-i+1}^{u_{FMA}}| + |\theta_{b-\{(j-1) \bmod b\}+b*(q-\max(2,i)+1)}^{\bar{u}(i)}| |\theta_{q-i+1}^{u_{FMA}}| |y_j|,$$

holds with probability at least $1 - \{(1 - p_b(\lambda, \bar{u}, c_1)) + (1 - p_b(\lambda, u_{FMA}, c_2))\}$, where $c_1 \triangleq b - ((j-1) \bmod b) + b*(q - \max(2, i) + 1)$ and $c_2 \triangleq q - i + 1$. We can obtain the upper bound for $i = j = 1$ (for which $\theta_{\zeta}^{\bar{u}}$ is effectively $\theta_{\zeta-1}^{\bar{u}}$ since $\delta_{j=1}^{i=1} = 0$) then relax the bounds to obtain $|\tilde{\theta}_{b-\{(j-1) \bmod b\}+b*(q-\max(2,i)+1)}^{\bar{u}}| \leq \tilde{\gamma}_{n-1}^{\bar{u}}$ and $|\tilde{\theta}_{q-i+1}^{u_{FMA}}| \leq \tilde{\gamma}_q^{u_{FMA}}$. Thus,

$$|\Delta y_j| \leq (\gamma_{n-1}^{\bar{u}} + \gamma_q^{u_{FMA}} + \gamma_{n-1}^{\bar{u}} * \gamma_q^{u_{FMA}}) |y_j|.$$

The forward error bound for matrix-matrix multiplication is then given as stated in theorem 3.9.

Theorem 3.9 (Tensor cores without representation error). *Let $\mathbf{D} = \mathbf{AB}$ be computed using Tensor Cores, where \mathbf{A}, \mathbf{B} are given in the floating point system t_{low} . If algorithm 1 is used to compute the matrix-matrix multiplication, then under lemma 2.2, the computed approximation $\hat{\mathbf{D}}$ satisfies*

$$\frac{|\hat{\mathbf{D}} - \mathbf{D}|}{|\mathbf{D}|} \leq (\gamma_{n-1}^{\bar{u}} + \gamma_q^{u_{FMA}} + \gamma_{n-1}^{\bar{u}} * \gamma_q^{u_{FMA}}) \frac{|\mathbf{A}||\mathbf{B}|}{|\mathbf{AB}|}$$

holds with a probability of at least

$$1 - m * t \left(\sum_{i=1}^q \sum_{j=(i-1)b+1}^{ib} 2 - p_b(\lambda, \bar{u}, c_1) - p_b(\lambda, u_{FMA}, c_2) \right),$$

where $c_1 \triangleq b - ((j-1) \bmod b) + b * (q - \max(2, i) + 1)$ and $c_2 \triangleq q - i + 1$.

In the case where \mathbf{A} and \mathbf{B} are given in a floating point system t^* with unit roundoff $u < u_{low}$, then we must account for the initial change in precision. Using lemma 2.2 we can obtain

$$\tilde{\mathbf{D}} = (\mathbf{A} + \Delta\mathbf{A})(\mathbf{B} + \Delta\mathbf{B}), \quad |\Delta\mathbf{A}| \leq u_{low}|\mathbf{A}|, |\Delta\mathbf{B}| \leq u_{low}|\mathbf{B}|,$$

which always holds. This gives the computed approximation to \mathbf{D} as

$$\begin{aligned} \hat{\mathbf{D}} &= (\mathbf{A} + \Delta\mathbf{A})(\mathbf{B} + \Delta\mathbf{B}) + \Delta\mathbf{P}; \quad |\Delta\mathbf{P}| \leq (\tilde{\gamma}_{n-1}^{\bar{u}} + \tilde{\gamma}_q^{u_{FMA}} + \tilde{\gamma}_{n-1}^{\bar{u}} * \tilde{\gamma}_q^{u_{FMA}}) |\mathbf{A} + \Delta\mathbf{A}| |\mathbf{B} + \Delta\mathbf{B}|, \\ &= \mathbf{AB} + \mathbf{A}\Delta\mathbf{B} + \Delta\mathbf{A}\mathbf{B} + \Delta\mathbf{A}\Delta\mathbf{B} + \Delta\mathbf{P} \\ &\triangleq \mathbf{AB} + \Delta\mathbf{E}, \end{aligned}$$

where $\Delta\mathbf{P} \triangleq \mathbf{A}\Delta\mathbf{B} + \mathbf{A}\Delta(\mathbf{B} + \Delta\mathbf{B}) + \Delta\mathbf{A}\mathbf{B} + \Delta\mathbf{A}\Delta\mathbf{B} + \Delta\mathbf{A}\Delta(\mathbf{B} + \Delta\mathbf{B})$ which we can bound to obtain the forward error bounds. This is stated in theorem 3.10.

Theorem 3.10 (Tensor cores with representation error). *Let $\mathbf{D} = \mathbf{AB}$ be computed using Tensor Cores, where \mathbf{A}, \mathbf{B} are given in the floating point system t^* with unit roundoff $u < u_{low}$. If algorithm 1 is used to compute the matrix-matrix multiplication, then under lemma 2.1, the computed approximation $\hat{\mathbf{D}}$ satisfies*

$$\frac{|\hat{\mathbf{D}} - \mathbf{D}|}{|\mathbf{D}|} \leq (2u_{low} + u^2 + \zeta(1 + u_{low})^2) \frac{|\mathbf{A}||\mathbf{B}|}{|\mathbf{AB}|},$$

holds with probability at least

$$1 - m * t \left(\sum_{i=1}^q \sum_{j=(i-1)b+1}^{ib} 2 - p_b(\lambda, \bar{u}, c_1) - p_b(\lambda, u_{FMA}, c_2) \right),$$

where $c_1 \triangleq b - ((j-1) \bmod b) + b * (q - \max(2, i) + 1)$, $c_2 \triangleq q - i + 1$, and $\zeta \triangleq (\tilde{\gamma}_{n-1}^{\bar{u}} + \tilde{\gamma}_q^{u_{FMA}} + \tilde{\gamma}_{n-1}^{\bar{u}} * \tilde{\gamma}_q^{u_{FMA}})$.

4. Numerical Experiments

In this section, we present the numerical experiments conducted on several kernels. First, we present the backward error bounds obtained in the case of the Multiply-Accumulate (MAC) unit. This kernel is fundamental to several kernels, such as dot-products and matrix-matrix products. We present the error bounds for performing the MAC operation using FMA and MPFMA operations. Following this, we present the forward error bounds in the case of matrix-matrix multiplication using TCs. For all error evaluations, computations using `fp64` are considered as the actual result.

4.1. Multiply-Accumulate (MAC) Unit

Consider the MAC operation $d = a \times b + c$, for which the computed approximation is given as \hat{d} . For a, b and c distributed uniformly as $\mathcal{U}[1, 2]$, the empirical distribution function (EDF) of the forward error and its bounds are shown in fig. 5. For a random variables X , the EDF is defined as $F_X(t) \triangleq \frac{1}{n} \sum_{i=1}^n \mathbf{1}_{X=x_i \leq t} \in [0, 1]$, where x_i denotes an observation of the random variable X and $\mathbf{1}$ is

an indicator function. Thus, if $F_{X_1}(t) < F_{X_2}(t)$, where X_1 and X_2 are random variables defined on the same support would mean that there is a larger probability that X_1 is less than t compared to X_2 . FMA operations result in smaller accumulated rounding errors, as observed by a smaller largest ϵ_{fwd} compared to the MAC operation without FMA operation. Mixed-precision introduces a larger backward error due to the initial change in representation from `fp32` to `fp16` for a and b . The forward error bounds from the deterministic analysis are tighter (estimates the largest ϵ_{fwd} well) compared to the probabilistic ones where MAC is computed without FMA and using MPFMA. This is expected for a small number of operations per floating point value, as shown in [23]. For FMA operations, as shown in section 3.1, DBEA and VIBEAs result in the same bounds that tightly estimate the accumulated error. Despite the larger accumulated error MPFMA, the low precision arithmetic results in smaller memory bandwidth consumption and larger arithmetic intensity, as tabulated in table 3.

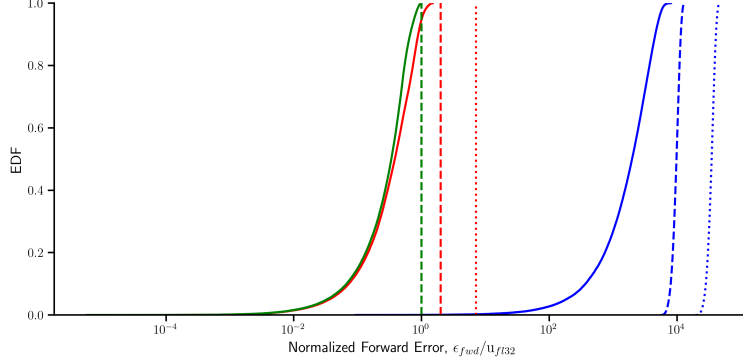


Figure 5: Empirical distribution for the forward error ($\frac{|\hat{d}-d|}{|d|}$) and its bounds for the MAC operation. True forward error for the MAC operation computed without FMA operation (—), with FMA operation (—), and with MPFMA operation (—). Deterministic analysis (DBEA) backward error bounds computed without FMA operation (---), with FMA operation (---), and with MPFMA operation (---). Probabilistic analysis (VIBEAs) backward error bounds computed without FMA operation (.....), with FMA operation (.....), and with MPFMA operation (.....). DBEA results in tighter estimates than VIBEAs in the case of without FMA and MPFMA. Both DBEA and VIBEAs estimate the backward error for the FMA operation tightly.

Algorithm	Arithmetic intensity [Flop/Byte]	Flops/s
MAC (W/o FMA)	0.00995	0.00004
MAC (W/ FMA)	0.00989	0.00004
MAC (W/ MPFMA)	0.02442	0.00008

Table 3: MAC operation profile

4.2. Matrix-Matrix Multiplication using Tensor Cores

Consider the matrix-matrix multiplication $\mathbf{D} = \mathbf{AB}$, where $\mathbf{A} \in \mathbb{R}^{m \times t}$, $\mathbf{B} \in \mathbb{R}^{t \times n}$, and $\mathbf{D} \in \mathbb{R}^{m \times n}$. We consider the case where $m = 2^{10}$, $t = 2^{15}$, and $n = 2^3$, where the elements of the matrices are drawn from the uniform distribution $\mathcal{U}(-1, 1)$. We use the cuBLAS library on an NVIDIA H100 GPU to compute the matrix-matrix multiplication using Tensor Cores. The code snippet for the matrix-matrix multiplication is provided in Algorithm 1. The empirical distribution of the forward error ($\frac{|\hat{d}-d|}{|d|}$) and its bounds for the matrix-matrix multiplication are shown in Figure 6. Storing the matrices in `fp16` and performing MPFMA, the maximum forward error is bounded by $u_{fp32} \times 10^{11} \approx \mathcal{O}(10^2)$ using DBEA and $\mathcal{O}(10^1)$ using VIBEAs. The VIBEAs bounds are tighter than the DBEA bounds by nearly an order of magnitude. However, both DBEA and VIBEAs bounds are loose compared to the actual maximum forward error, which is $\mathcal{O}(10^{-2})$. While DBEA assumes the worst-case scenario, which will always overestimate the error, VIBEAs bounds can be improved by considering more informative rounding error distributions.

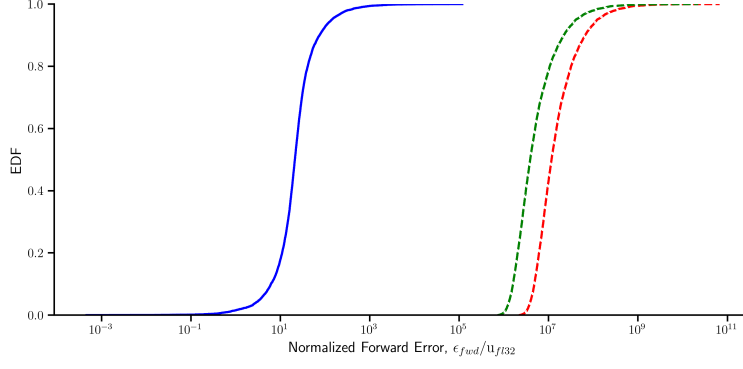


Figure 6: Empirical distribution for the forward error ($\frac{|\hat{d}-d|}{|d|}$) and its bounds for matrix-matrix multiplication ($m = 2^{10}, t = 2^{15}, n = 2^3$) using Tensor Cores. True forward error for the multiplication (—). Bounds obtained using DBEA (---) and VBEA (---). VBEA bounds are tighter than DBEA bounds by nearly an order of magnitude.

Listing 1: Matrix-matrix multiplication using Tensor Cores.

```

1 // cuBLAS handle
2 cublasHandle_t handle;
3 cublasCreate(&handle);
4 int alpha = 1;
5 int beta = 0;
6 int lda = m; // Leading dimension of a
7 int ldb = t; // Leading dimension of b
8 int ldc = m; // Leading dimension of c
9 // Compute the matrix-matrix multiplication
10 cublasGemmEx(handle, CUBLAS_OP_N, CUBLAS_OP_N, m, t, n, &alpha, a, CUDA_R_16F,
    lda, b, CUDA_R_16F, ldb, &beta, c, CUDA_R_16F, ldc, CUDA_R_32F,
    CUBLAS_GEMM_DEFAULT_TENSOR_OP);
11 // Synchronize the device
12 cudaDeviceSynchronize();
13 // Destroy the cuBLAS handle
14 cublasDestroy(handle);

```

5. Concluding Remarks

In this work, we present rounding error analysis for fused multiply-accumulate (FMA), mixed-precision fused multiply-accumulate (MPFMA), and matrix-matrix multiply using Tensor Cores. These kernels are fundamental to numerical linear algebra and are widely used in scientific computing. Developing accurate error bounds for these kernels is important for understanding the impact of rounding errors on the accuracy of numerical computations. To this end, we present deterministic and probabilistic error bounds for these kernels to study the impact of rounding errors on large-scale computations. Through numerical experiments, we demonstrate that MPFMA results in nearly $\mathcal{O}(10^4)$ times larger error compared to FMA. However, this error comes at nearly two times increase in performance. We also show that for large-scale matrix-matrix multiplication TCs can produce reliable computations, with $\mathcal{O}(10^{-2})$ error in the case where data is distributed randomly as $\mathcal{U}(0,1)$. Probabilistic error bounds for matrix-matrix multiplication can produce nearly an order of magnitude improvement in estimating rounding errors compared to the deterministic analysis. However, both probabilistic and deterministic bounds overestimate the maximum error by nearly $\mathcal{O}(10^5)$.

Probabilistic analysis shows promise for estimating rounding error for large-scale computations. However, there is need to improve the modeling assumptions for rounding errors and using better inductive bias. For example, future work could consider the leveraging the empirical rounding error distributions proposed in recent work [26, 27].

Acknowledgments

This research was supported by the National Science Foundation grant FMITF-2219997 and by the Los Alamos National Laboratory grant titled ‘Algorithm/Hardware/Software Codesign for High Energy Density Applications.’

References

- [1] S. Gupta, A. Agrawal, K. Gopalakrishnan, P. Narayanan, Deep learning with limited numerical precision, in: International conference on machine learning, PMLR, 2015, pp. 1737–1746.
- [2] N. Wang, J. Choi, D. Brand, C.-Y. Chen, K. Gopalakrishnan, Training deep neural networks with 8-bit floating point numbers, *Advances in neural information processing systems* 31 (2018).
- [3] I. Hubara, M. Courbariaux, D. Soudry, R. El-Yaniv, Y. Bengio, Quantized neural networks: Training neural networks with low precision weights and activations, *Journal of Machine Learning Research* 18 (187) (2018) 1–30.
- [4] E. A. Paxton, M. Chantry, M. Klöwer, L. Saffin, T. Palmer, Climate modeling in low precision: Effects of both deterministic and stochastic rounding, *Journal of Climate* 35 (4) (2022) 1215–1229.
- [5] T. Kimpson, E. A. Paxton, M. Chantry, T. Palmer, Climate-change modelling at reduced floating-point precision with stochastic rounding, *Quarterly Journal of the Royal Meteorological Society* 149 (752) (2023) 843–855.
- [6] S. Hatfield, M. Chantry, P. Düben, T. Palmer, Accelerating high-resolution weather models with deep-learning hardware, in: *Proceedings of the platform for advanced scientific computing conference*, 2019, pp. 1–11.
- [7] N. J. Higham, S. Pranesh, M. Zounon, Squeezing a matrix into half precision, with an application to solving linear systems, *SIAM journal on scientific computing* 41 (4) (2019) A2536–A2551.
- [8] A. Haidar, H. Bayraktar, S. Tomov, J. Dongarra, N. J. Higham, Mixed-precision iterative refinement using tensor cores on gpus to accelerate solution of linear systems, *Proceedings of the Royal Society A* 476 (2243) (2020) 20200110.
- [9] A. Haidar, P. Wu, S. Tomov, J. Dongarra, Investigating half precision arithmetic to accelerate dense linear system solvers, in: *Proceedings of the 8th workshop on latest advances in scalable algorithms for large-scale systems*, 2017, pp. 1–8.
- [10] A. Abdelfattah, H. Anzt, E. G. Boman, E. Carson, T. Cojean, J. Dongarra, A. Fox, M. Gates, N. J. Higham, X. S. Li, et al., A survey of numerical linear algebra methods utilizing mixed-precision arithmetic, *The International Journal of High Performance Computing Applications* 35 (4) (2021) 344–369.
- [11] A. Buttari, J. Dongarra, J. Langou, J. Langou, P. Luszczek, J. Kurzak, Mixed precision iterative refinement techniques for the solution of dense linear systems, *The International Journal of High Performance Computing Applications* 21 (4) (2007) 457–466.
- [12] Y. Liu, X. Liu, E. Wu, Real-time 3d fluid simulation on gpu with complex obstacles, in: *12th Pacific Conference on Computer Graphics and Applications*, 2004. PG 2004. *Proceedings.*, IEEE, 2004, pp. 247–256.
- [13] P. R. Rinaldi, E. Dari, M. J. Vénere, A. Clausse, A lattice-boltzmann solver for 3d fluid simulation on gpu, *Simulation Modelling Practice and Theory* 25 (2012) 163–171.
- [14] M. Karp, F. Liu, R. Stanly, S. Rezaeiravesh, N. Jansson, P. Schlatter, S. Markidis, Uncertainty quantification of reduced-precision time series in turbulent channel flow, in: *Proceedings of the SC’23 Workshops of The International Conference on High Performance Computing, Network, Storage, and Analysis*, 2023, pp. 387–390.

- [15] G. Lienhart, A. Kugel, R. Manner, Using floating-point arithmetic on fpgas to accelerate scientific n-body simulations, in: Proceedings. 10th Annual IEEE Symposium on Field-Programmable Custom Computing Machines, IEEE, 2002, pp. 182–191.
- [16] N. J. Higham, Accuracy and stability of numerical algorithms, SIAM, 2002.
- [17] J. Von Neumann, H. H. Goldstine, Numerical inverting of matrices of high order (1947).
- [18] T. E. Hull, J. R. Swenson, Tests of probabilistic models for propagation of roundoff errors, Communications of the ACM 9 (2) (1966) 108–113.
- [19] P. Henrici, Test of probabilistic models for the propagation of roundoff errors, Communications of the ACM 9 (6) (1966) 409–410.
- [20] M. Tienari, A statistical model of roundoff error for varying length floating-point arithmetic, BIT Numerical Mathematics 10 (3) (1970) 355–365.
- [21] I. C. Ipsen, H. Zhou, Probabilistic error analysis for inner products, SIAM journal on matrix analysis and applications 41 (4) (2020) 1726–1741.
- [22] N. J. Higham, T. Mary, Sharper probabilistic backward error analysis for basic linear algebra kernels with random data, SIAM Journal on Scientific Computing 42 (5) (2020) A3427–A3446.
- [23] S. Bhola, K. Duraisamy, Variance-informed rounding uncertainty analysis for floating-point statistical models, arXiv preprint arXiv:2404.12556 (2024).
- [24] IEEE, Ieee standard for floating-point arithmetic, ieee std 754-2019 (revision of ieee 754-2008), Institute of Electrical and Electronics Engineers New York, 2019.
- [25] P. Blanchard, N. J. Higham, F. Lopez, T. Mary, S. Pranesh, Mixed precision block fused multiply-add: Error analysis and application to gpu tensor cores, SIAM Journal on Scientific Computing 42 (3) (2020) C124–C141.
- [26] F. Dahlqvist, R. Salvia, G. A. Constantinides, A probabilistic approach to floating-point arithmetic, in: 2019 53rd Asilomar Conference on Signals, Systems, and Computers, IEEE, 2019, pp. 596–602.
- [27] Y. Fang, L. Chen, Probabilistic rounding error analysis from a statistical perspective, arXiv preprint arXiv:2405.07537 (2024).